

CCD photometry of the Tucana dwarf galaxy *

Ivo Saviane¹, Enrico V. Held², and Giampaolo Piotto¹

¹ Università di Padova, Dipartimento di Astronomia, vicolo dell’Osservatorio 5, I-35122 Padova, Italy

² Osservatorio Astronomico di Bologna, via Zamboni 33, I-40126 Bologna, Italy

Abstract. We present V and I CCD photometry for ~ 360 stars in the recently discovered dwarf galaxy Tucana. The large field investigated and the accurate photometric calibration make our data complementary to the deeper HST photometry. From the I magnitude of the tip of the red giant branch we estimate a distance modulus $(m - M)_0 = 24.69 \pm 0.16$, corresponding to 870 ± 60 Kpc, confirming that Tucana is an isolated dwarf spheroidal located almost at the border of the Local Group. From the color of the red giant branch tip and by direct comparison with the giant branches of galactic globular clusters we estimate a metallicity $[\text{Fe}/\text{H}] = -1.8 \pm 0.2$, with no clear indication for a metallicity spread. The color-magnitude diagram indicates that Tucana has had a single star formation burst at the epoch of the Galactic globular cluster star formation. There is no evidence for an intermediate or young stellar population. We derive the V luminosity profile, the surface density profile of resolved stars, and the structural parameters of Tucana, from which we confirm that Tucana participates to the general metallicity-surface brightness-absolute magnitude relations defined by the Galaxy and M31 dwarf spheroidal and dwarf elliptical companions.

Key words: Galaxies: fundamental parameters – **Galaxies: individual: Tucana** – Local Group – Galaxies: stellar content – Galaxies: structure

1. Introduction

Among the 12 known dwarf spheroidal (dSph) galaxies in the Local Group (LG), nine (including the recently discovered Sagittarius dwarf; Ibata et al. 1994) are in the halo of the Milky Way, three are companions to the Andromeda Galaxy, and only one, Tucana, is far from any luminous member of the LG. The properties of the LG are the subject of recent reviews, e.g., Caldwell (1995), Da Costa (1994), Gallagher & Wyse (1994), and Zinn (1993). The isolated location of Tucana offers a unique opportunity to study the evolution of dwarf galaxies in an environment different from the halo of giant spiral galaxies and to constrain models for their formation.

Send offprint requests to: E. V. Held

*Based on data collected at the European Southern Observatory, La Silla, Chile

Tucana, although already present in the Southern Galaxy Catalog (Corwin et al. 1985), was overlooked for some time before its serendipitous re-discovery by Lavery (1990). Lavery & Mighell (1992) presented a shallow $V - (V - I)$ color-magnitude diagram (CMD) based on low-resolution imaging reaching $V \sim 23$. They suggested the classification of this galaxy as a dE5 dwarf spheroidal in the LG, and an upper limit of 24.75 mag for the distance modulus. No direct metallicity determination was given.

Preliminary photometric results have been reported by Da Costa’s (1994) in his recent review. He obtained a $V - (B - V)$ color-magnitude diagram showing neither young blue stars nor very red, bright stars that might indicate the presence of a conspicuous intermediate-age population, from which Tucana seems to be indistinguishable from the dSph companions to our Galaxy and M31. By fitting the giant branches of M92, M3, and 47 Tuc to the data, he obtained $(m - M)_0 = 24.8 \pm 0.2$ mag and a metallicity $[\text{Fe}/\text{H}] = -1.8 \pm 0.25$ dex, the distance error being the largest contributor to the uncertainty in the abundance. Da Costa (1994) also presented a B surface brightness profile of Tucana showing no indication for sub-structure in the star distribution. An exponential law fit to the data yields a scale length $\alpha = 30''$ (geometric mean radius) or 130 pc at a distance of 900 kpc, an extrapolated central surface brightness $\mu_{0,B} = 25.5$ mag arcsec $^{-2}$, and an absolute magnitude $M_V = -9.3 \pm 0.4$.

The first results of an ongoing deep HST imaging study of Tucana by Seitzer and coll. (see Caldwell 1995) are a color-magnitude diagram with no evidence for young stars, and a moderately blue horizontal branch (HB). Since Tucana has a metallicity as low as $[\text{Fe}/\text{H}] = -1.8$ (a value confirmed by this study), one might expect an even bluer HB, and the authors suggest that a mild second parameter effect may be present (cf. e.g., Leo II: Demers S. & Irwin 1993). Castellani M. et al. (1995) presented a progress report of a study using the same data (obtained from the HST archive), and deep ground-based CCD observations. They obtain a distance modulus consistent with that of Da Costa (1994), and marginally higher metallicity ($[\text{Fe}/\text{H}] = -1.56 \pm 0.20$), and claim that the spread in color on the RGB is larger than the one expected on the basis of photometric errors.

In order to provide clues as to whether the star formation history and structure of dwarf spheroidals are affected by environment, we present a comprehensive CCD study of the stellar populations and structure of Tucana, based on V, I CCD photometry over a relatively wide field of 5.7×5.7 . This area allows

a complete coverage of the galaxy. Photometry of the stars in our field provides a well populated upper RGB, essential for obtaining reliable distance and metallicity estimates. The plan of the present paper is as follows. Observations and stellar photometry are described in Sec. 2. Sect. 3 presents the $I - (V - I)$ color-magnitude diagrams of Tucana. A new accurate distance determination is derived in Sec. 4 by locating the RGB tip on the I luminosity function. New estimates for the mean metal abundance and abundance spread of stars on the red giant branch (RGB) are presented in Sec. 5. Surface photometry is presented in Sec. 6 where structural and photometric parameters are derived. In Sec. 7 we discuss the properties of Tucana in the framework of the general relations for dwarf elliptical and spheroidal galaxies.

2. Observations and data reduction

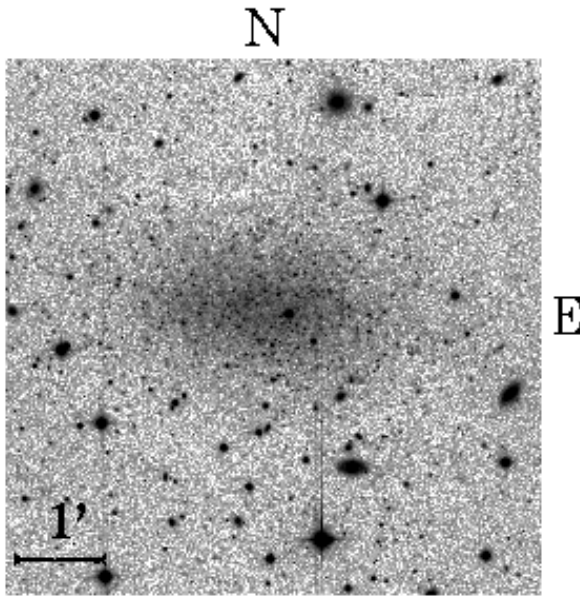


Fig. 1. The combined V image of Tucana from our data with good seeing

Observations were obtained in two runs, on September 15-16, 1993 and September 2-3, 1994, using EFOSC2 at the ESO 2.2m telescope. EFOSC2 was equipped with a 1024×1024 pixels Thomson coated CCD (ESO #19); the pixel size was $19 \mu\text{m}$ yielding a scale $0''.336 \text{ pixel}^{-1}$ and a field of view $5''.7 \times 5''.7$. The CCD conversion factor was $2.1 \text{ e}^-/\text{ADU}$, and the read-out noise, measured from the overscan region, was 4 e^- (cf. EFOSC2 User Manual).

Weather conditions and seeing were quite variable during both runs, so the quality of the observations is not uniform. A journal of the observations selected for this study is given in Table 1. The useful images have been grouped into two sets: the first set includes the best images ($\text{FWHM} \leq 1.2''$), most of which were taken on the single best night of Sept. 3, 1994 (under photometric conditions). A second set includes all the images taken in medium, yet acceptable, seeing conditions ($\sim 1''.5$ FWHM). All images with seeing worse than $1.5''$ FWHM have been discarded.

Table 1. The journal of observations

<i>N</i>	filter	<i>t_{exp}</i>	Date	UT	<i>X</i>	FWHM
1	V	1800	1993 Sept. 15	01:40	1.32	$1.4''$
2	I	2700	1993 Sept. 15	02:15	1.27	$1.5''$
3	V	1800	1993 Sept. 15	03:09	1.23	$1.3''$
4	I	2700	1993 Sept. 15	03:44	1.22	$1.5''$
5	V	1800	1994 Sept. 3	00:58	1.52	$1.2''$
6	I	1800	1994 Sept. 3	01:33	1.42	$1.2''$
7	I	1800	1994 Sept. 3	02:06	1.35	$1.5''$
8	V	1800	1994 Sept. 3	02:46	1.29	$1.5''$
9	V	1800	1994 Sept. 3	03:19	1.26	$1.5''$
10	I	1800	1994 Sept. 3	03:55	1.23	$1.2''$
11	I	1800	1994 Sept. 3	04:29	1.22	$1.1''$
12	I	1800	1994 Sept. 3	05:02	1.23	$1.2''$
13	V	1800	1994 Sept. 3	05:42	1.25	$1.2''$

Processing of the CCD frames was accomplished as follows. First, a constant offset was determined from the overscan region and subtracted from each frame (sample bias frames are constant across the chip and stable in time). Both sky and dome flat-fields (the latter taken on a white screen illuminated by day light) were taken in the 1994 run. A comparison of dome and sky flats shows them to be consistent at the 1% level. For the 1994 observations, master twilight-sky flats have been created for each filter, with residual stellar images removed by taking the median of individual exposures. For the 1993 run only dome flats were available.

After preliminary processing, the frames were sorted by filter and by seeing quality. Images from the “good seeing” set and the “medium seeing” set were carefully registered to a common reference frame. Finally, the registered frames were co-added, yielding four master images, and the $1.2''$ *V* image is shown in Fig. 1. The size of the Point Spread Function (PSF) on the combined images shows no degradation with respect to the individual frames.

Stellar photometry was performed using DAOPHOT and ALLSTAR (Stetson 1987, 1994) in the MIDAS environment. After a few experiments, we found that an analytic Moffat function (with $\beta = 2.5$), along with a variable PSF model with quadratic dependence on distance from the frame center, provided the best representation of the PSF. A PSF was iteratively constructed for each master frame starting with a set of ~ 50 bright, non-saturated stars and progressively reducing this sample to ~ 20 stars by discarding poorly fit stars. In particular, visual inspection of a PSF image created by adding an artificial star to an empty frame was employed to identify and reject any PSF stars contaminated by faint components. ALLSTAR was run twice on the combined frames, using our best PSF and the aperture photometry catalogs. For each of the four combined images, all stars detected and analyzed on the first run of ALLSTAR were subtracted and the residual images searched again for faint undetected objects. Then, ALLSTAR was run again on the complete list of stars.

In order to analyze the degree of completeness and the photometric errors as a function of magnitude and location

on the frame, artificial star experiments were performed using the DAOPHOT task ADDSTAR, along with a code written by one of us (I.S.) to perform automatically the individual experiments as well as the general program of simulations. Each experiment follows a scheme designed to yield approximately constant number of stars per magnitude bin. The results of these simulations are summarized in Table 2: columns 1 and 2 specify the central magnitude of the V bins and mean colors, columns 3 to 5 are the standard deviations in V , I , and $(V-I)$, column 6 to 8 give the number of stars added (N_i) for each magnitude bin, the completeness ratio $c = N_f/N_i$ (where N_f is the number of artificial stars eventually found and measured by DAOPHOT), and its standard error. Magnitude (color) errors have been derived from the rms scatter of the difference between input and measured magnitudes (colors) of the artificial stars. Finally, σ_c has been estimated from the scatter of c obtained from 10 individual experiments at a fixed magnitude. Completeness is ~ 1 for $V \leq 20.7$ and falls below 20% for $V \geq 24.2$.

Table 2. Photometric errors and incompleteness

V	$(V-I)$	σ_V	σ_I	$\sigma_{(V-I)}$	N_i	N_f/N_i	σ_c
21.24	1.60	0.014	0.010	0.021	300	0.99	0.03
21.74	1.51	0.021	0.017	0.030	420	0.99	0.02
22.23	1.42	0.028	0.028	0.045	800	0.99	0.03
22.73	1.33	0.041	0.044	0.071	1240	0.98	0.03
23.22	1.21	0.071	0.068	0.093	2060	0.95	0.03
23.71	1.09	0.108	0.109	0.153	2500	0.84	0.04
23.96	1.02	0.110	0.159	0.193	220	0.64	0.09

Star-like objects were selected out of the raw photometric catalogs by using a set of selection criteria based on the values of the DAOPHOT parameters related to the quality of the fit and image shape (χ and *sharp*). The distribution of the same parameters resulting from artificial star experiments served as a training set, complemented by careful scrutiny of the Tucana co-added images. Objects with $\chi > 1.5$ turned out to be hot pixels (mostly cosmic rays) or spikes around bright sources; similarly, objects with *sharp* < -1 are isolated hot pixels while *sharp* > 1 corresponds to PSF spikes and diffuse objects.

Absolute calibration is based on observations of Landolt's (1992) standard stars on the photometric night of Sept. 3, 1994. We have obtained the following calibrations (standard deviations of the residuals are 0.006 mag in V and 0.014 mag in I , respectively):

$$V = v' + 0.053(V-I) + 23.69 \quad (1)$$

$$I = i' - 0.055(V-I) + 22.47 \quad (2)$$

where v' , i' are instrumental magnitudes defined as follows:

$$m' = m_{\text{ap}} + 2.5 \log(t_{\text{exp}} + \Delta t) - k_{\lambda} X. \quad (3)$$

m_{ap} are the “total” magnitudes resulting from a growth-curve analysis of the standard stars in circular apertures up to a radius $R = 6''.4$ (we have verified that magnitudes measured within larger apertures, say $R \leq 10''$, are only 0.01 mag brighter on the average). Δt is the average shutter delay and k_{λ} represents the extinction coefficients in the V , I bands. For the shutter delay we have assumed 0.4 s (Veronesi 1995); assuming $\Delta t = 0$ would not affect the $(V-I)$ color measurements, while V , I magnitudes would be fainter by 0.02 mag. We used mean extinction coefficients for La Silla $k_V = 0.14$ and $k_I = 0.06$, obtained from photoelectric photometry on the standard Johnson/Bessel system at La Silla (G. Clementini, priv. comm.). These values are confirmed by the La Silla Extinction database of the Geneva Observatory. A plausible $\pm 10\%$ fluctuation of extinction during the night may contribute about ± 0.02 mag to the zero point uncertainty on the V and I magnitudes, and less than 0.005 mag to the $V - I$ color uncertainty.

The aperture corrections needed to transform the PSF magnitudes of the Tucana stars into “total” aperture magnitudes, were then calculated as mean differences (C_V and C_I) between raw PSF-fit magnitudes and the instrumental magnitudes, for the set of bright, isolated stars on reference images of Tucana taken on the photometric night of Sept. 3, 1994. We paid particular attention to avoid systematic errors on the colors, and found that the instrumental colors of the reference stars are almost independent of aperture size (with an rms error of 0.004 mag) for radii $3''.0 < R < 6''.4$ (magnitudes measured in larger apertures become more affected by background noise). To assess the systematic accuracy of the calibrated magnitudes and colors, we compared the instrumental magnitudes v' , i' of the reference stars from *all* the individual images of Tucana taken on the photometric night of Sept. 3, 1994. Table 3 lists the values of the zero-point constants C_V and C_I for all the individual calibration frames. The C_V , C_I values show some scatter (0.01 mag in V and 0.02 mag in I , 1σ errors), but no obvious dependence on seeing. This scatter includes, in addition to uncertainties on aperture correction, the errors on shutter timing and extinction corrections. These errors, together with the uncertainty on the calibration relations, yield a 0.01 mag zero-point rms uncertainty in the V band, and 0.02 mag in the I band. The corresponding uncertainty on the $V - I$ color is 0.03 mag.

Table 3. Zero point shifts as determined from different images

N	filter	FWHM	airmass	C_{λ}
6	I	1.2	1.42	7.56
7	I	1.5	1.35	7.57
10	I	1.2	1.23	7.63
11	I	1.1	1.22	7.63
12	I	1.2	1.23	7.64
5	V	1.2	1.52	7.48
8	V	1.5	1.29	7.50
9	V	1.5	1.26	7.48
13	V	1.2	1.25	7.53

3. Color-magnitude diagrams

In order to reduce the effects of field contamination on the color-magnitude diagrams and luminosity functions, we defined an “inner region” (or “galaxy region”) including all stars within an ellipse (area 5.8 arcmin²) with semi-major axis $a = 108''$ and a provisional axial ratio $b/a = 0.56$ (adopting the axial ratio determined in Sec. 6 would not change our results). Similarly, we defined an “outer region” of our frame (area 20.8 arcmin²) external to an ellipse with $a = 161''$.

The color-magnitude diagrams of Tucana are shown in Fig. 2 and Fig. 4, where V and I magnitudes are plotted against the $V - I$ color; Fig. 3 shows the $I - (V - I)$ color-magnitude diagram for the stars in the outer region. The red giant branch of Tucana is similar to the giant branch of old, metal-poor Galactic globular clusters. In the same figures, the Tucana’s CMD is compared with the $M_I - (V - I)_0$ diagrams of 6 globular clusters from Table 10 of Da Costa & Armandroff (1990; hereafter DA90), suitably scaled to the distance of Tucana. The average metal abundance of Tucana is clearly in the range $-2.17 < [\text{Fe}/\text{H}] < -1.54$.

The color-magnitude diagram of Fig. 3 is fairly representative of the background and foreground contamination, although Tucana extends to the outer region. The surface density Σ of objects in the outer region is $\sim 14\%$ that in the galaxy region (65.2 and 9.0 objects/arcmin², respectively). The expected ratio, as estimated for an exponential luminosity profile with scale length $30'' \pm 3''$ (see Sect. 6), is $\Sigma_{\text{out}}/\Sigma_{\text{in}} = 0.024 \pm 0.008$ (the error is obtained from the scale length uncertainty). From this ratio and the object counts, it is easy to estimate the contributions of galaxy stars and foreground/background objects in each region. It turns out that the surface density of background objects is $\Sigma_{\text{bkg}} = 7.6$ objects/arcmin², i.e. 84% of the objects in the outer region are due to background/foreground, while the contamination of the inner sample is at the 12% level.

An estimate of the expected Galactic star density towards Tucana was obtained from the Bahcall & Soneira’s (1980) model (see also Bahcall 1986 and references therein). The “export code” was modified to have $(V - I)$ as the output color instead of the original $(B - V)$. The main modification was the replacement of the globular and open cluster fiducial loci in $V - (B - V)$ with the corresponding $I - (V - I)$ loci. These loci have been obtained as follows: (a) the Population I Main Sequence (MS) from Girardi et al. (1996); (b) the disk Population MS and the M67 MS from Carraro et al. (1994); and (c) the GC’s sequences from Bergbush & Vandenberg (1992) isochrones, where the $(V - I)$ colors have been calculated by means of Kurucz (1991) model atmospheres. The $A_V/E_{(V-I)}$ ratio was adopted from Savage & Mathis (1979). In the outer region, the color and magnitude distributions are consistent with model expectations above the RGB tip ($V \simeq 22$), while there is a significant overabundance of objects with respect to the model counts for $V > 22$ (by a factor of 2–3).

However, in the magnitude interval shown in Fig. 2 some contamination of background galaxies is expected. According to Tyson’s (1988) galaxy counts, we expect ~ 90 objects for $20 < I < 22$. In the outer region, there are 86 stars in this range. According to the previous discussion, 72 of these should be foreground/background objects. In the same area and magnitude interval, we expect 26 foreground stars on the basis of the Bahcall and Soneira’s (1980) model. Therefore, about 46 objects should be background unresolved galaxies. This num-

ber is smaller than expected by Tyson’s (1988) counts; on the other hand, both the DAOPHOT task FIND and our rejection criteria tend to reject fuzzy not-star-like objects, and it is plausible that a fraction of the background galaxies has been rejected by the PSF-fitting routine, as demonstrated by a visual inspection of the star-subtracted image.

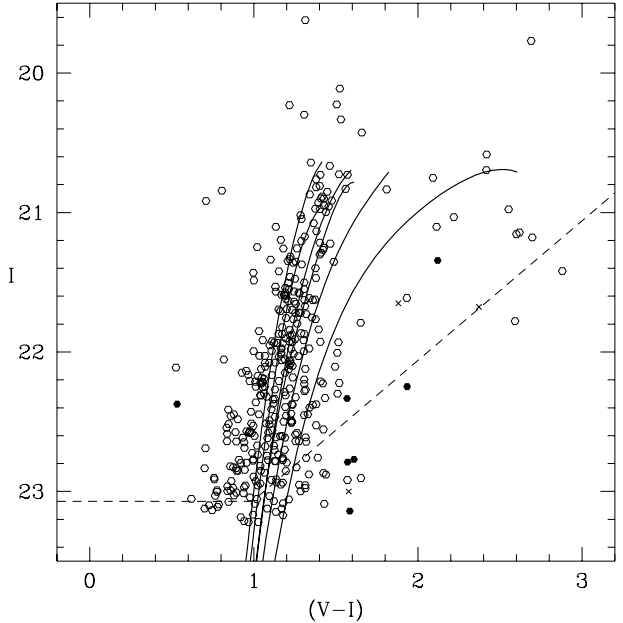


Fig. 2. The Tucana’s CMD, compared with globular cluster giant branches from Da Costa & Armandroff (1990). Open circles represent starlike objects; obvious faint galaxies are indicated by filled symbols, while crosses identify photometric blends; the *dashed line* represents the 50 % completeness level. Globular cluster fiducial loci are shifted to the same distance modulus as Tucana, assuming $(m - M) = 24.69$ and $A_I = E_{(V-I)} = 0$. Left to right: M15 ([Fe/H] = -2.17), NGC 6397 ([Fe/H] = -1.91), M2 ([Fe/H] = -1.58), NGC 6752 ([Fe/H] = -1.54), NGC 1851 ([Fe/H] = -1.29) and 47 Tuc ([Fe/H] = -0.71).

A fiducial line through the RGB has been derived by analyzing the color distributions in different magnitude bins. The magnitude range of each bin, the modal $(V - I)$ color, and the color dispersion $\sigma_{(V-I)}$, are given in Table 4 for both the 1''.2 image and the 1''.5 images. Column 5 will be described in detail in Sec. 5. The modal color represents the mode of the $(V - I)$ distribution, after all the outlier stars have been removed by an interactive procedure equivalent to a 3σ clipping. A linear interpolation of our fiducial RGB is $(V - I)_{\text{RGB}} = -0.187 I_{\text{RGB}} + 5.312$. Also the trend of the color spread as a function of magnitude was smoothed by fitting a linear relation to $\sigma_{(V-I)}$ vs. I : $\sigma_{(V-I)} = 0.058 I - 1.087$.

Stars within 2σ from the ridge line of the Tucana’s RGB define a clean sample of stars most likely belonging to Tucana (hereafter referred to as “ 2σ ” sample). For the “ 2σ ” sample, there are 339 and 87 objects in the inner and outer region, or $\Sigma_{\text{out}}/\Sigma_{\text{in}} = 0.07$, indicating that there is some contamination due to foreground/background objects, but that this is less than 5% (cf. previous discussion and Table 5).

We note a few starlike objects in the CMD at $(V - I) > 2$, just above the V completeness limit. Visual inspection of

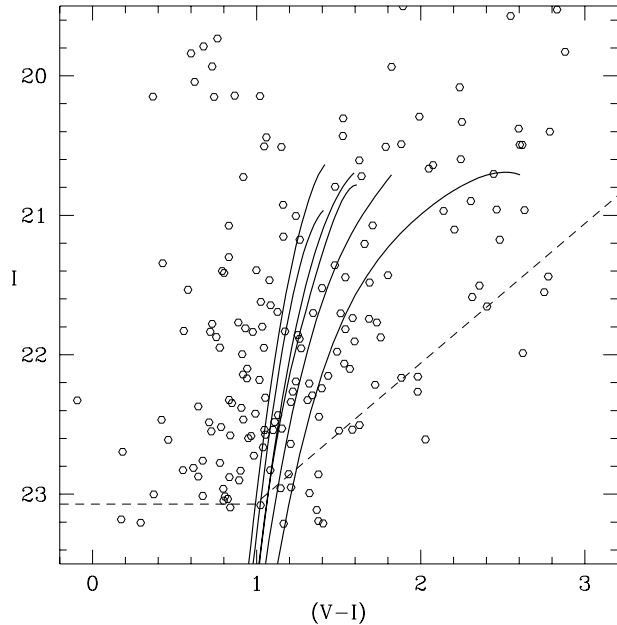


Fig. 3. As for Fig. 2, for the outer field

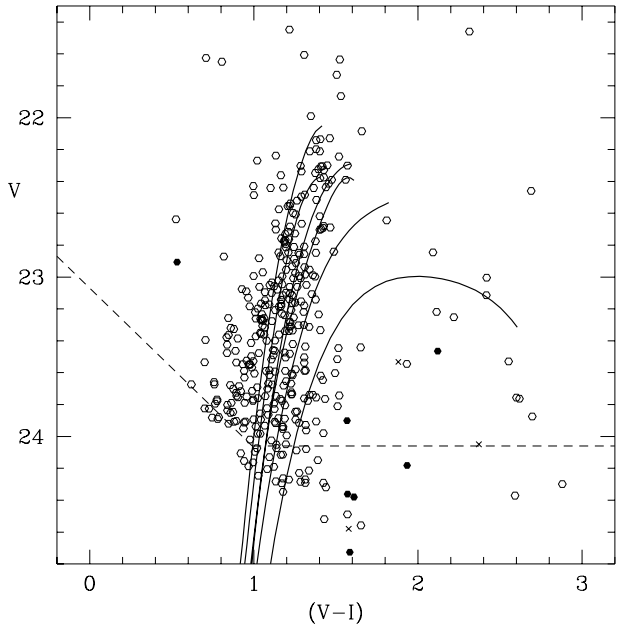


Fig. 4. As for Fig. 2, for V vs. $(V - I)$

Table 4. Fiducial sequence along the RGB

I	$(V - I)$	$\sigma_{(V-I)}(1''2)$	$\sigma_{(V-I)}(1''5)$	σ_{meas}
21.0–22.0	1.22	0.10	0.13	0.10
22.0–22.5	1.16	0.14	0.11	0.13
22.5–23.0	1.06	0.18	0.18	0.11

these stars allows us to rule out that they are artifacts near the limit of our photometry. Although there are a few obvious faint galaxies (filled symbols in Fig. 2), or photometric blends (crosses), most of the red objects appear to be star-like. It is of interest to understand whether these objects are red stars belonging to Tucana, since in that case they might indicate the presence of a metal-rich component. There are 15 red ($V - I > 2.0$) objects in the inner region and 35 in the outer region. Assuming for Tucana an exponential profile implies an excess of 5.3 ± 4.2 objects in the inner region, which is significant only at the 1σ level. We conclude that there is no significant population of red objects in Tucana.

As already noted by Da Costa (1994), another feature in the CMD of Fig. 2 is the absence of any significant number of stars bluer than the RGB. Lavery & Mighell (1992) noted a concentration of stars at $(V - I) \sim 1$, $V \sim 22$ in their color-magnitude diagram. These may be part of an asymptotic giant branch or, as the authors point out, just a manifestation of their large photometric color errors. Our CM diagrams confirm the latter explanation: there is no excess of stars bluer than $(V - I) = 1$ at the level of the RGB tip. More quantitatively, in the inner region there are 8 stars with $22 < V < 22.6$ and $(V - I) < 1.2$, while 14 stars are found in the outer re-

gion within the same magnitude and color ranges. Taking into account the expected surface density ratio of Tucana stars, we find that 6 out of the 8 stars are due to foreground/background contamination, and conclude that the number of stars bluer than $V - I = 1.2$ in Fig. 2 (or Fig. 4) is consistent with contamination alone.

Bright AGB stars belonging to an intermediate-age stellar population are quite common in dSph's (e.g., Freedman 1994). In order to set an upper limit to a younger stellar component in Tucana, we have estimated the number of stars brighter than the RGB tip in excess over the field contamination. The bolometric absolute magnitude of the brightest AGB stars is $M_{\text{bol}} = -3.8$ and $M_{\text{bol}} = -4.6$ for a 10 Gyr and 3 Gyr population, respectively, according to the relation between AGB tip luminosity and age given in Mould & Da Costa (1988) (cf. also the models of Bressan et al. 1994). These correspond, for the Tucana's metallicity, to $M_I = -4.3$ and $M_I = -5.1$. Therefore, adopting a distance modulus $(m - M) = 24.7$, AGB stars older than 3 Gyr and younger than 10 Gyr would be found in the range $19.6 < I < 20.4$. Counting stars in this magnitude range for the Tucana's inner and outer samples, we have found 7 stars in the inner region and 16 in the outer region (corresponding to 4.5 when scaled to inner area). Thus in the galaxy region there is an excess of 2.5 ± 2.9 stars brighter than the RGB tip (1σ Poisson error). If we limit ourselves to stars redder than the RGB tip ($V - I > 1.4$) the numbers are 4 and 7 stars, respectively, yielding an excess of 2.0 ± 2.1 stars. Visual inspection of the objects brighter than the RGB tip in the galaxy region shows that at least one has an elongated shape suggesting it is a blend or a background galaxy. Thus we conclude that the surface density of stars brighter than the RGB tip is entirely consistent with the star counts in the outer region over the same magnitude range, and rule out any significant population of AGB stars younger than 10 Gyr in Tucana.

4. Luminosity function and distance

Assuming that Tucana does not contain very red stars, we have derived the V and I RGB luminosity functions (LF) using stars in the 2σ sample, with a correction for incompleteness in both V and I according to the results of artificial star experiments and a correction for background/ foreground objects. The field object counts (properly scaled to the inner area) were obtained by counting stars in the outer field, applying the same color selection as for the inner field, and allowing for the 16% of the stars which represent the estimated contribution of Tucana stars in the outer region (cf. Sect. 3). The corrected LF's are shown in Fig. 5, and listed in Table 5 for the I magnitude and Table 6 for the V magnitude.

Table 5. RGB I luminosity function

I	N	N_{bkg}	c	N_c	σ_{N_c}
20.1	1.0	0.0	0.99	1.0	1.0
20.3	2.0	0.2	0.99	1.8	1.4
20.5	1.0	0.2	0.99	0.8	0.9
20.7	6.0	0.7	0.98	5.4	2.4
20.9	15.0	0.2	0.98	15.1	4.1
21.1	7.0	0.7	0.97	6.5	2.7
21.3	18.0	0.2	0.97	18.4	4.6
21.5	21.0	0.7	0.96	21.1	5.0
21.7	22.0	1.6	0.95	21.3	5.0
21.9	30.0	2.3	0.95	29.1	6.0
22.1	34.0	1.9	0.95	33.8	6.5
22.3	37.0	2.3	0.94	36.7	7.0
22.5	36.0	3.7	0.90	35.9	7.3
22.7	39.0	1.2	0.79	48.0	9.4
22.9	38.0	2.8	0.61	57.3	12.2
23.1	26.0	1.9	0.42	57.2	16.2

Table 6. RGB V luminosity function

V	N	N_{field}	c	N_c	σ_{N_c}
21.7	2.0	0.0	0.99	2.0	1.4
21.9	2.0	0.5	0.99	1.6	1.3
22.1	5.0	0.2	0.98	4.8	2.3
22.3	18.0	1.2	0.98	17.2	4.4
22.5	16.0	0.5	0.97	16.0	4.3
22.7	21.0	0.7	0.97	21.0	5.0
22.9	28.0	1.9	0.96	27.3	5.8
23.1	39.0	2.6	0.95	38.3	6.9
23.3	43.0	2.1	0.95	43.0	7.5
23.5	36.0	4.2	0.94	33.9	6.8
23.7	50.0	3.3	0.85	54.9	9.6
23.9	43.0	1.6	0.65	63.6	12.5

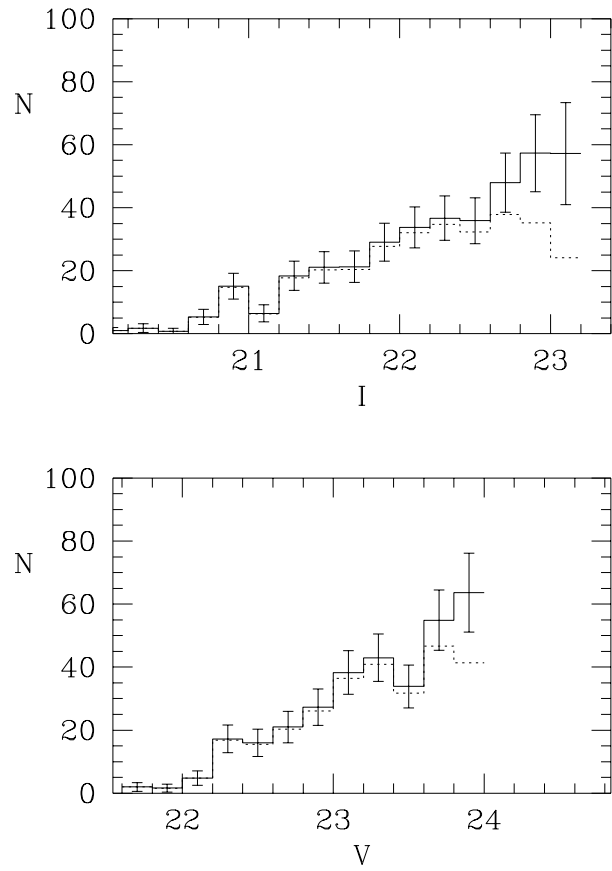


Fig. 5. V and I luminosity functions before (dotted lines) and after (solid lines) completeness corrections and field object subtraction

Figure 6 shows the RGB luminosity function of Tucana along with the LF of Fornax (Sagar et al. 1990). In the same figure, the LF of Tucana is also compared with the theoretical LF from Bergbush & VandenBerg (1992) for a metal abundance $[\text{Fe}/\text{H}] = -1.68$ ($Z = 0.0004$). In Fig. 7 we compare the

observed V absolute magnitude of the RGB tip, M_V^{TRGB} , with the V luminosity of the RGB tip from the Bergbush & Vandenberg's (1992) models, for different ages and metallicities, assuming a distance of 870 pc (see below). M_V^{TRGB} is a sensitive function of metallicity, becoming fainter as the metal content grows, while it is little sensitive to age for stellar populations older than 8 Gyr (in contrast, the LF can be a useful age indicator for younger stellar populations). If Tucana's dominant population is similar to old globular clusters (a plausible assumption given the absence of any significant intermediate-age population), the location of the observed tip (shaded region in Fig. 7) is consistent with models with $Z = 0.0004$ ($[\text{Fe}/\text{H}] = -1.68$), in very good agreement with the metallicity estimates given in Sect. 5.

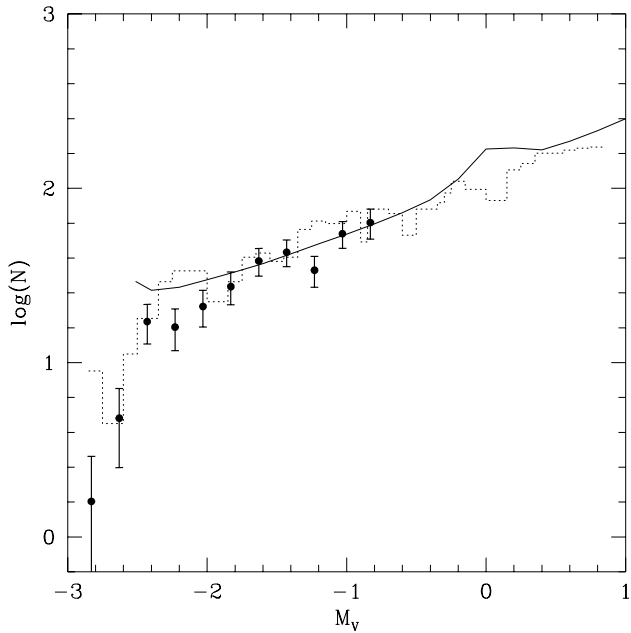


Fig. 6. Tucana's LF (dots with error bars) compared to that of Fornax (dotted histogram; Sagar et al. 1990), and to a theoretical LF (solid line; models from Bergbush & Vandenberg 1992, with $Z = 0.0004$ and Age = 15 Gyr)

The I magnitude of the tip of the first-ascent red giant branch can be used to determine the distance to Tucana, following the methods described in Mould & Kristian (1986) and Lee et al. (1993a). Distance estimates obtained using the RGB tip have been shown to be of comparable accuracy to using Cepheid or RR Lyrae variables (Madore & Freedman 1995). This method has the considerable advantage that for old, metal-poor systems ($-2.2 < [\text{Fe}/\text{H}] < -0.7$, $2 < t < 15$ Gyr), the I absolute magnitude of the RGB tip is almost independent of abundance ($M_I \simeq -4.0 \pm 0.1$ mag), so that mutually independent distance and metallicity estimates can be obtained. Following Lee et al. (1993a), the RGB tip was measured by convolving the I luminosity function with a zero-sum Sobel kernel; the result of the convolution with the edge detector is shown in Fig. 8. The RGB tip is evident at $I = 20.7$, with an estimated uncertainty of the order 0.15 mag.

The distance was then calculated from the I absolute magnitude of the RGB tip, using the relations of DA90 yielding the

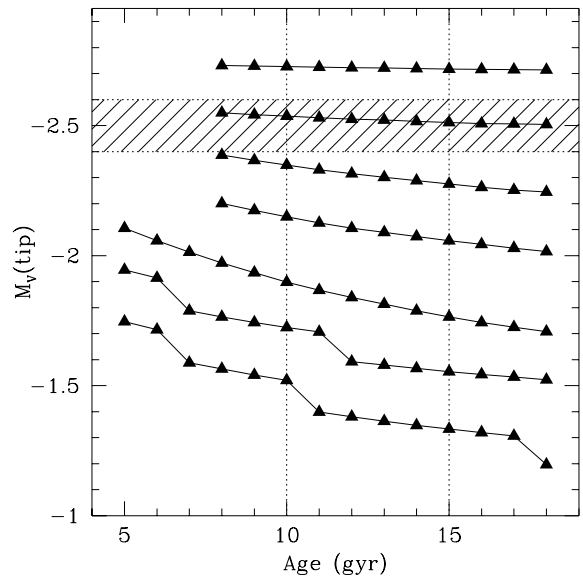


Fig. 7. V absolute luminosity of the RGB tip in the Bergbush & Vandenberg (1992) model isochrones, for different ages and metallicities. The shaded region indicates the absolute magnitude and uncertainty of the Tucana's RGB tip, after correction for distance modulus. Data points connected by solid lines represent models with fixed metallicity (top to bottom: $Z = 0.0001, 0.0004, 0.001, 0.002, 0.003, 0.004, 0.006$)

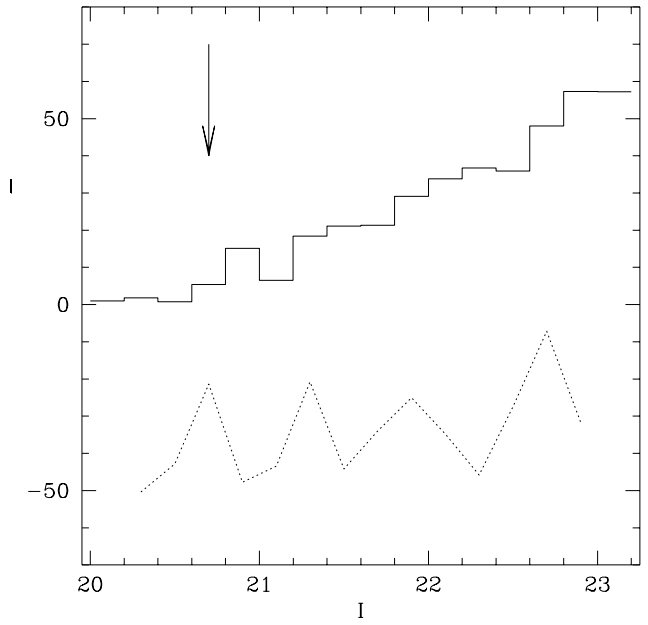


Fig. 8. The I luminosity function of Tucana (solid line) is convolved with an edge-detector to find the RGB tip (dotted line). The tip is clearly seen at $I = 20.7 \pm 0.15$

bolometric luminosity of the RGB tip as a function of metallicity, and the bolometric correction as a function of color:

$$BC_I = 0.881 - 0.243(V - I)_{\text{tip}} \quad (4)$$

$$M_{\text{bol}} = -0.19 \text{ [Fe/H]} - 3.81. \quad (5)$$

Assuming $[\text{Fe/H}] = -1.82$ for the metallicity (cf. Sec. 5), and $(V - I)_{\text{tip}} = 1.45 \pm 0.05$ (cf. Fig. 2), we obtain $BC_I = 0.531 \pm 0.01$, $M_{\text{bol}}^{\text{TRGB}} = -3.46 \pm 0.04$, $M_I^{\text{TRGB}} = -3.99 \pm 0.04$, and $M_V^{\text{TRGB}} = -2.54 \pm 0.04$. The distance modulus to Tucana is then $(m - M) = 24.69 \pm 0.16$, corresponding to 870 ± 60 kpc.

5. Metallicity

5.1. Mean abundance

We have estimated the metallicity of Tucana using two different procedures, both based on the globular cluster data of Da Costa & Armandroff (1990). First, the abundance has been estimated from $(V - I)_{-3.5}$, the color of the RGB measured at absolute magnitude $M_I = -3.5$, using the relation

$$[\text{Fe/H}] = -12.64 + 12.6(V - I)_{-3.5} - 3.3(V - I)_{-3.5}^2 \quad (6)$$

(Lee et al. 1993a).

$(V - I)_{-3.5}$ was obtained from a 3σ -clipped Gaussian fit to the color distribution of the giant stars in the range $21.13 < I < 21.33$. The distribution is peaked at $(V - I)_{-3.5} = 1.31 \pm 0.03$ (standard error of the mean), yielding $[\text{Fe/H}] = -1.82 \pm 0.12$. The reddening towards Tucana is $E_{(B-V)} = 0.00 \pm 0.01$ (Burstein & Heiles 1982), so that absorption and reddening corrections are negligible.

Second, the metallicity of Tucana was determined by direct comparison of the Tucana's RGB with the globular cluster giant branches of DA90. The mean color differences $\delta(V - I)_0$ between the RGB sequences of the 6 GC's in Fig. 2 and our Tucana's giant branch have been calculated using the brightest 1.8 mag of the sequence ($I \leq 22.5$). The color differences are plotted in Fig. 9 against globular cluster metallicities.

In order to reduce the statistical noise, we used only stars in the 2σ sample. A linear fit to the mean color differences as a function of GC metallicities on the DA90 system is

$$\delta(V - I)_0 = -0.274 \text{ [Fe/H]} - 0.498. \quad (7)$$

The interpolated metal abundance of Tucana is $[\text{Fe/H}] = -1.81$, with a dispersion about the regression line $\sigma_{(V - I)} = 0.01$ (standard deviation of the mean). Adding quadratically the systematic uncertainty 0.03 mag on the absolute color calibration, we obtain a total uncertainty $\sigma[\delta(V - I)] = 0.03$, and $\sigma[\text{Fe/H}] = 0.11$ dex for the metallicity error. This error must be considered as an internal error, intrinsic to the method we have adopted to estimate the metallicity. A further error source comes from the uncertainty in the distance modulus. Assuming a distance modulus error of 0.16 mag (cf. Sec. 4), we have further an uncertainty of ± 0.13 on $[\text{Fe/H}]$. To these error sources, we need to add the intrinsic uncertainty in the GC metallicity, which is of the order of ± 0.1 dex (Zinn and West 1984), making the total uncertainty for Tucana's metallicity of 0.20 dex.

Since stars on the red and asymptotic giant branches cannot be separated with the present photometric errors (≤ 0.2

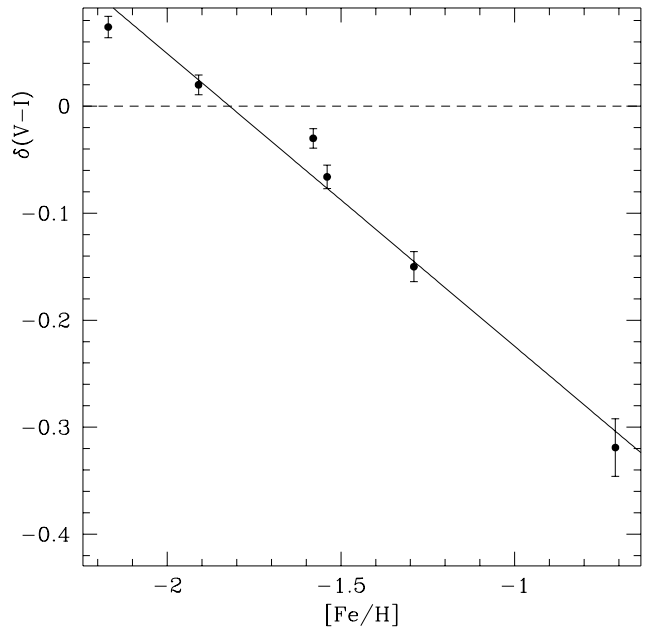


Fig. 9. The mean difference between Tucana's fiducial RGB points and fiducial RGB lines from Da Costa & Armandroff (1990) is plotted against $[\text{Fe/H}]$. The error bars are the standard deviations of the residuals in $(V - I)$. The solid line represent a linear fit to the points (see text)

mag), we discuss here a possible bias introduced by the presence of the old-population AGB. The brightest AGB stars are found 1.2 and 1.4 mag below the RGB tip in the $I - (V - I)$ color magnitude diagrams of M15 and M2, respectively. Since the metallicity of Tucana is intermediate between that of M15 ($[\text{Fe/H}] = -2.17$) and M2 ($[\text{Fe/H}] = -1.58$), we assume that the upper 1.3 mag of the Tucana's RGB is unaffected by AGB stars, under the hypothesis that the bulk of its stellar population is similar to that of old globular clusters. Therefore, we have repeated the interpolation using the brightest 1.2 mag of the giant branch, and selecting only stars with $(V - I) > 1.15$, and found $[\text{Fe/H}] = -1.83$. We conclude that the average metallicity of Tucana is $[\text{Fe/H}] = -1.82 \pm 0.20$ and adopt this value in the present paper.

5.2. RGB width

The RGB color spread of several dwarf spheroidals has been found to be larger than measurement errors, a result generally interpreted as due to an abundance spread of the red giant population. This is not a general rule, however. For instance, Smecker-Hane et al. (1994) have been able to separate the contributions of the RGB and the intermediate-age AGB found in Carina, suggesting that the width of the giant branch is consistent with the RGB of Galactic globular clusters. The presence of a metal-abundance spread has received in some cases spectroscopic confirmation, e.g., from spectrophotometry of individual giants in Draco (Lehnert et al. 1992) and Sextans (Suntzeff et al. 1993). For example, from a model atmosphere analysis of 14 giants in Draco, Lehnert et al. (1992) conclude that the color spread of Draco's giants is due to a ~ 1 dex range in metal abundance. Such a range of chemical abun-

dance is traced back to chemical enrichment of the interstellar medium by supernova ejecta and stellar winds.

Here we have measured the RGB width from our photometry to see if it is compatible with internal errors. Clearly, tighter upper limits on an intrinsic abundance dispersion are expected from HST observations. Fig. 10 shows the width of the RGB as measured from the 1''.2 and the 1''.5 image sets. The two sets give similar results. By comparing the colors from the two sets, we have obtained an estimate of the internal errors which is independent of an AGB contribution to the color spread. In a given magnitude bin, we have calculated $\sigma_{\Delta(V-I)}$, the standard deviation of the difference between the color measurements of the same stars in the two image sets. This reflects the combined measurements errors. Assuming that the color measurements are of comparable uncertainty in the two image sets, and uncorrelated, we can estimate the color measurement error $\sigma_{\text{meas}} = \sigma_{\Delta(V-I)}/\sqrt{2}$. The values of σ_{meas} are listed in Table 4 and plotted in Fig. 10, whereas the 1σ color errors derived from artificial star experiments on the 1''.2 data are listed in Table 2. While, in principle, crowding experiments (which use a constant PSF) could underestimate the random measurement errors in the case of large PSF variations across the frame, in the present case random errors estimated from simulations and from comparison of different frames are perfectly consistent. Note that the low value of σ_{meas} for the faintest bin is an artifact of incompleteness in the 1''.5 frames.

As shown in Fig. 10, the RGB width is consistent with the measurement errors σ_{meas} . Thus, our data indicate that the color spread of Tucana's giant branch is not significantly different from that expected on the basis of photometric errors. Once measurement errors are critically and carefully assessed, no convincing indication of an abundance spread is found in our data.

6. Surface photometry and structural parameters

6.1. Surface photometry

In this section we derive the structural parameters of Tucana needed to compare this galaxy with the other LG dwarf spheroidals. Our procedure follows quite closely the methods of Caldwell et al. (1992). In order to measure the luminosity profile of Tucana, all stars brighter than $I = 20$ or redder than $V - I = 1.84$ were subtracted from the coadded images using DAOPHOT. Further, all bright stars, obvious background galaxies, and diffraction spikes were interactively masked out. In this way we were left with stars mostly belonging to the RGB, superimposed onto a diffuse, unresolved light component. Surface photometry was performed only on the V image, since flat-fielding of the outermost area of the I image was not of sufficient accuracy to derive an extended surface brightness profile. The cleaned master V image was processed as follows. After 2×2 rebinning, the frame was median filtered with a 5×5 box. The smoothed image thus produced is essentially elliptical, with intrinsic noise due to the presence of resolved stars with a distribution which appears somewhat clumpy. Ellipses were fit to isophotes in the radial range $37'' < a < 138''$ (a being the semi-major axis), leaving all parameters free. Given the noise on the parameters of each ellipse, we restrict ourselves to providing mean values of ellipticity ($\epsilon = 1 - b/a$) and position angle (PA) for $a > 65''$. These are given in Table 7 along with their standard errors.

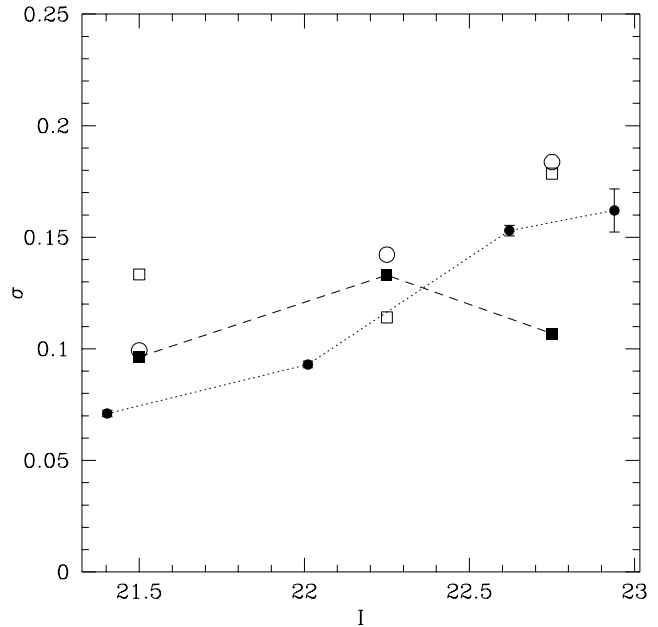


Fig. 10. The color spread of the Tucana's giant branch for the 1''.2 set (open circles) and the 1''.5 set (open squares) is plotted along with σ_{meas} , the instrumental dispersion in $(V - I)$ derived from the color differences for stars in both data sets (filled squares). Also plotted is the standard deviation in $(V - I)$ from artificial star experiments on the 1''.2 coadded image (dots)

A V surface brightness profile including galaxy + sky was then obtained as the median flux along ellipses with constant ellipticity and orientation, and plotted against geometric radius ($r_g = \sqrt{ab}$). The azimuthally averaged profile is essentially flat for $r_g > 140''$, so that the mean intensity for $r_g > 140''$ was chosen to represent the sky level. In this range, the rms scatter of the profile, binned in $10''$ intervals, is $\sim 0.05\%$. Large-scale ($> 20''$) peak-to-valley fluctuations of the sky background in the master V frame, in the absence of azimuthal averaging, are of the order 0.3% . By extrapolating the inner ($r_g < 100''$) exponential profile out to this geometric radius, we estimate that the galaxy light at $r_g = 140''$ is of the order 0.1% of (or about $7.5 \text{ mag arcsec}^{-2}$ below) the sky background. This is comparable to the uncertainties on the sky level, and the profile can be reliably measured down to $\mu_V \sim 29 \text{ mag arcsec}^{-2}$, where the galaxy light contribution becomes comparable to 3σ sky fluctuations. The sky-subtracted V luminosity profile of Tucana is shown in Fig. 11 against geometric radius, along with an exponential fit in the range $10'' - 100''$. As it is common for dwarf elliptical galaxies (cf. Caldwell et al. 1992), the surface brightness profile of Tucana is well fit by an exponential law except for the center.

The scale length (α) and central extrapolated surface brightness of the fit ($S_{0,V}$) are specified in Table 7, assuming a distance of 870 kpc. Note that all magnitude errors given in Table 7 reflect internal error estimates; a 0.02 mag zero point uncertainty should be added to account for systematic errors. Our best fit gives a scale length of $29'' \pm 5''$, or 123 pc. This scale length is consistent with that found by Da Costa (1994), and makes Tucana one of the smallest dwarf spheroidals known.

Table 7. Structural parameters for Tucana

Parameter	Value	
V_T	15.15	\pm 0.28
M_V	-9.55	\pm 0.34
$\mu_{0,V}$ (obs)	25.05	\pm 0.06
α (pc)	123	\pm 21
$S_{0,V}$	24.31	\pm 0.25
R_e (pc)	205	\pm 36
SB_e	25.43	\pm 0.27
r_c (pc)	176	\pm 26
r_s (pc)	166	\pm 14
$\mu_{0,V}$ (King)	24.76	\pm 0.15
c	0.72	\pm 0.21
$1 - b/a$	0.48	\pm 0.03
P.A.	97°	\pm 2°

Our extrapolated central surface brightness $S_{0,V} = 24.3$ mag arcsec $^{-2}$ is somewhat brighter than that measured by Da Costa (24.8 mag arcsec $^{-2}$ assuming a central color $B - V = 0.7$). The error estimates given in Table 7 were obtained from the 90% confidence intervals for one interesting parameter. Similar errors on the parameters of the exponential fit (and derived parameters) result from assuming a sky level uncertainty of $\pm 1\%$, three times larger than the sky fluctuations.

The total magnitude of Tucana ($V_T = 15.15 \pm 0.28$) was calculated by integrating the observed surface brightness profile in the innermost region ($0'' < r_g < 20''$), and adding a correction based on the exponential fit. Alternatively, V_T was obtained from the observed profile alone, integrated out to $r_g = 150''$, in which case the asymptotic value is $V_T = 15.05$. The two methods give consistent results within the quoted errors. The absolute magnitude $M_V = -9.6$ mag is consistent, within the large uncertainties inherent in this kind of measurements for dwarf spheroidals, with the values derived by previous authors. The effective geometric radius R_e , as well as SB_e , the mean surface brightness inside R_e , were derived from the parameters of the exponential fit. The errors on all derived quantities were obtained by assigning their extreme values to $S_{0,V}$ and α . In the case of M_V we have also taken into account a 0.2 mag error on the distance modulus.

As shown in Fig. 12, a King law is also well fit to the Tucana surface brightness profile (we used in this case the same radial range as for the exponential fit). The King fit parameters were estimated as follows. First, a fit was obtained allowing all parameters to vary. This yielded the central surface brightness of the fit profile, $\mu_{0,V} = 24.76$ mag arcsec $^{-2}$ (not to be confused with the intensity scale parameter of the King law), the “core radius” r_s , and the concentration parameter c , all listed in Table 7. For comparison, the core radius at which the surface brightness drops at half the central value is $r_c = 42'' \pm 6''$ (176 ± 26 pc). Then, a King law with a fixed concentration $c = 0.75$ was used to derive the uncertainties on $\mu_{0,V}$ and r_s from the 90% confidence ranges of the fit for one interesting parameter. Likewise, the uncertainty on c was obtained by repeating the fit with a fixed value for $\mu_{0,V}$. An alternative estimate of the uncertainties of the parameters was obtained

by changing the sky level by $\pm 3\sigma$. The effect is comparable to or less than the internal errors of the fit: ± 0.12 mag on surface brightness, ± 0.09 for c , and a negligible effect for r_s .

Also in the case of the King fit, the central surface brightness of the fit profile, $\mu_{0,V}$ (King), is higher than the observed value, $\mu_{0,V}$ (obs) = 25.05 ± 0.06 mag arcsec $^{-2}$. The latter was calculated as the median surface brightness in the inner $3''$, together with its associated rms scatter. The dip is certainly real, since it is also seen in the I profile, and the B profile of Da Costa (1994). Inspection of the images seems to suggest a clumpy (“ring-like”) distribution of the bright giants in the central region, rather than evidence of a dust lane.

Finally, Fig. 13 shows the integrated color of Tucana inside $r_g = 40''$. The central $(V - I) = 0.89 \pm 0.01$ was obtained as the mean of the inner $20''$ ($V - I = 0.87$ inside $40''$). Adopting the mean relation $(B - V) = 0.8(V - I)$ derived for the giant branches of globular clusters (see Smecker-Hane et al. 1994), this value corresponds to $(B - V) = 0.70$, in full agreement with the result of Da Costa (1994).

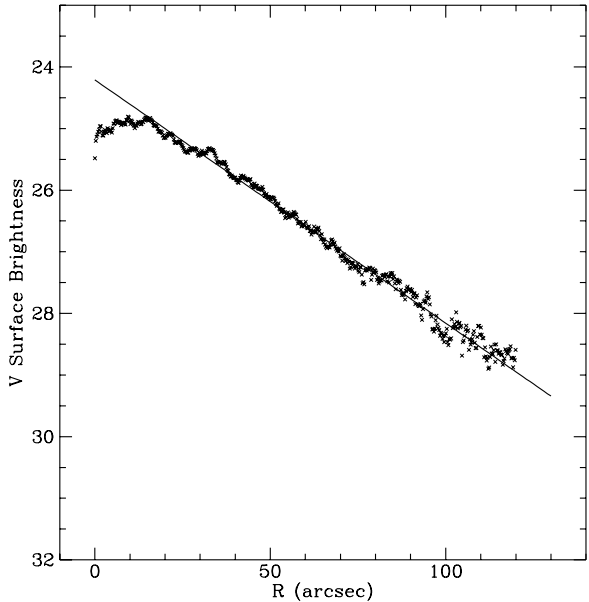


Fig. 11. Surface brightness in V (mag arcsec $^{-2}$) against the geometric radius for Tucana. The line represents an exponential fit to the luminosity profile between $15''$ and $100''$, with scale length $31''$

6.2. Surface density of resolved stars

We have also investigated the structure of Tucana using the surface density of stars as a function of distance from the galaxy center. Figure 14 shows the surface density profile obtained by counting stars in elliptical annuli with a $5''$ step in semi-major axis, and fixed ellipticity and position angle. Only stars in the magnitude range $20.7 < I < 22.5$ have been considered. The counts have been corrected for the radially varying incompleteness. The background+foreground counts have been estimated from the count level beyond $200''$ to be 7.6 ± 1.0 arcmin $^{-2}$ (standard deviation refers to the mean value of 29 bins). The small number of stars inside a $10''$ radius is only partially explained by incompleteness. An exponential fit to the

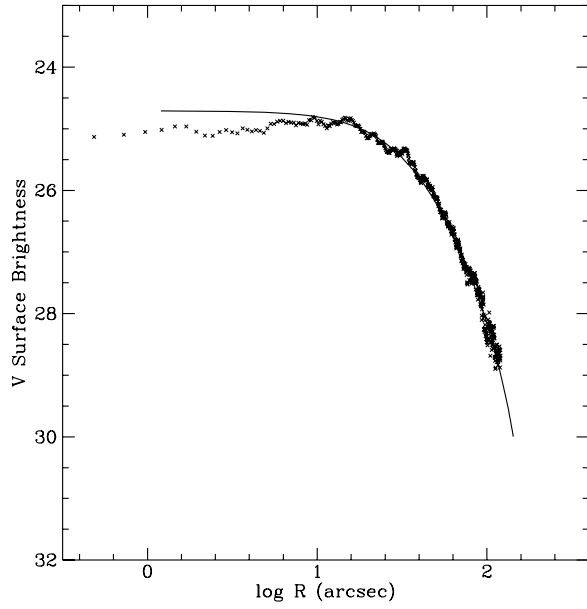


Fig. 12. King law fit to the Tucana's equivalent V luminosity profile, with core radius $39''$ and concentration parameter 0.72

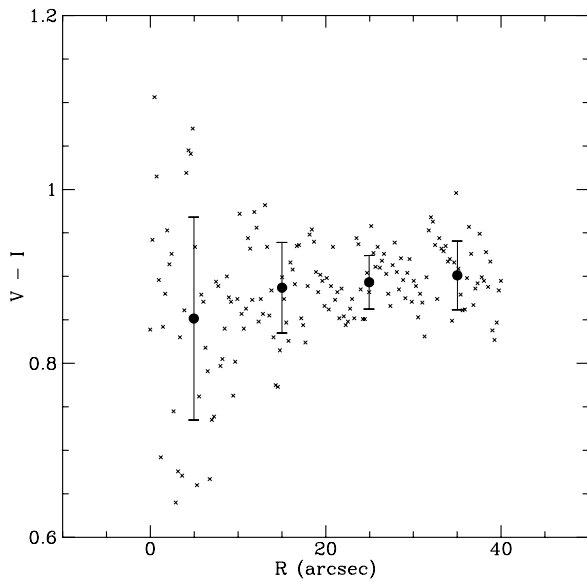


Fig. 13. Median $(V - I)$ color averaged on ellipses plotted against distance from the galaxy center. Dots with error bars represent mean values in $10''$ bins

counts between $20''$ and $90''$ yields a scale length $\alpha = 31'' \pm 3''$ (131 ± 13 pc), in good agreement with the results from surface photometry. The uncertainty has been estimated by empirically varying the background value by $\pm 5\sigma$ and repeating the fit in the same radial interval.

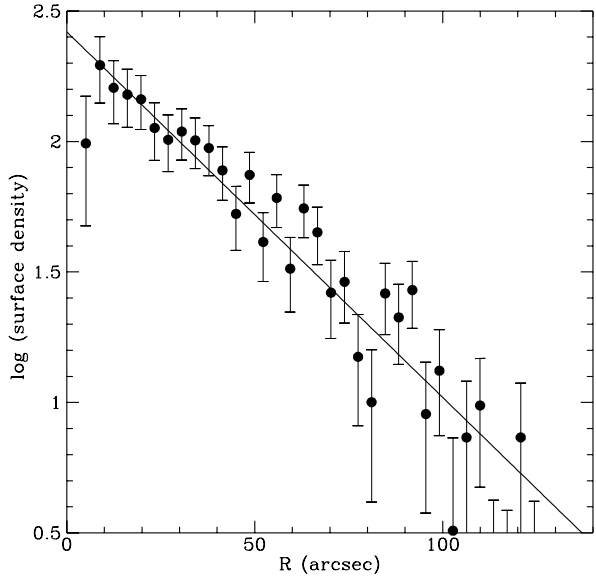


Fig. 14. Surface density (arcmin^{-2}) of resolved stars in the Tucana field. Abscissa is geometric radius. Also shown is an exponential fit with scale length $29''$ (solid line)

6.3. Absolute magnitude from the LF

The completeness-corrected V luminosity function has also been used to estimate the absolute magnitude M_V of Tucana by comparison with the LF of the globular cluster M3. The corrected V luminosity function given in Table 6 was scaled by a factor 1.20 to match the luminosity function of M3 from Sandage (1954). The logarithmic shift is 0.083 ± 0.055 (the error being the standard deviation of the differences on a logarithmic scale).

Since the magnitude distribution in Table 6 refers to the inner region, an extrapolation factor to total counts over the entire galaxy was obtained by integrating the surface brightness profile. Assuming that the luminosity profile of Tucana follows an exponential law with a $30''$ scale length, we find that the inner region contains $\sim 73\%$ of the Tucana stars. Further, we assume that 5% of the RGB stars are left out from the 2σ -sample. Therefore the number of stars in the Tucana's LF should be multiplied by 1.45, so that $L_{\text{Tuc}} = L_{\text{M3}} * 1.75$. Assuming $M_V^{\text{M3}} = -8.75$ (Djorgovski 1993), we obtain for Tucana $M_V = -9.4 \pm 0.28$, in very good agreement with the absolute magnitude estimate given in Sect. 6.1. The errors are estimated taking into account the rms uncertainty in the sliding fit of the LF's, a 10% uncertainty on the scale length, and the uncertainty on the distance modulus.

7. Discussion

Deep color-magnitude diagrams obtained in the last decade have revealed a wide variety of star formation histories in dwarf spheroidals, and direct evidence for recent star formation has been found in 50% of the dE/dSph galaxies in the LG (Freedman 1994). A complex star formation history seems also to be fairly common in Virgo and Fornax dE's (see Ferguson & Binggeli 1994; Held & Mould 1994; and references therein). The presence of carbon stars in many dSph companions to the Galaxy, and in And II, (see Armandroff 1994 for a recent review) indicates that star formation took place over an extended time period, probably in episodes alternated to quiescent phases.

A possible correlation between the star formation history of dSph and their distance from the parent galaxy was noted by van den Bergh (1994), in the sense that young or intermediate-age populations are preferentially found in dSph's far from the Milky Way. He suggested that dSph close to the Galaxy formed the bulk of their stars at early epochs, either because efficient star formation was triggered by interaction, or because any remaining gas was efficiently removed by supernova-driven winds or high UV flux. According to this trend, a distant dwarf such as Tucana would be expected to harbour an intermediate-age population, witnessing a continued history of star formation, as in Carina (e.g., Smecker-Hane et al. 1994) and Leo I (Lee et al. 1993b).

Our study confirms that Tucana is located in a no-man's-land, close to the border of the LG, at 870 Kpc from the Galaxy and ~ 1300 Kpc from both M31 and M33. There are other isolated dwarf galaxies in the LG (e.g., Phoenix, WLM, NGC 6822, DDO 210, etc...): all of them have experienced recent star formation. As suggested by Da Costa (1994) and shown in Sec. 3, there is no sign of intermediate or young population in the color-magnitude diagram of Tucana, thus Tucana does not follow the proposed trend of the star formation history in the LG galaxies. This absence of an intermediate-age population seems to imply that galactic winds expelled the interstellar medium at early epochs and halted star formation, a process apparently not dependent on environment. One further question rises immediately: is Tucana an unique example or are there many other dwarf spheroidals located far from the largest galaxies in the Local Group ? Clearly, the discovery of dwarf galaxies located in the outer parts of the LG is biased in favour of star forming objects. On the other hand, at distances beyond 400–500 Kpc and out to the borders of the LG (~ 1 Mpc), identifying new dSphs like Tucana is extremely difficult with the current survey techniques (Irwin 1994), and the search must be considered highly incomplete.

While Tucana is peculiar as far as its star formation history is concerned, in many other respects it is indistinguishable from other LG dSphs or dEs. It does not contain large amounts of HI, though the 3σ non-detection upper limit of $M_{HI}/L_B < 2.5$ (Lavery and Michell 1992) still corresponds to $\sim 10^6 M_\odot$, and a better estimate of the HI content would be needed. Tucana's morphological parameters are within the range of the Galaxy and M31 dSph companions, and it conforms to the surface brightness–absolute magnitude–metallicity relations defined by the LG dSph (cf. Da Costa 1994). In Fig. 15 we have plotted the effective surface brightness for the dSphs of the LG against their absolute magnitude. Tucana clearly lies on the single relation defined by the Milky Way and M31 companions (Caldwell et al. 1992). The surface brightness seems to be

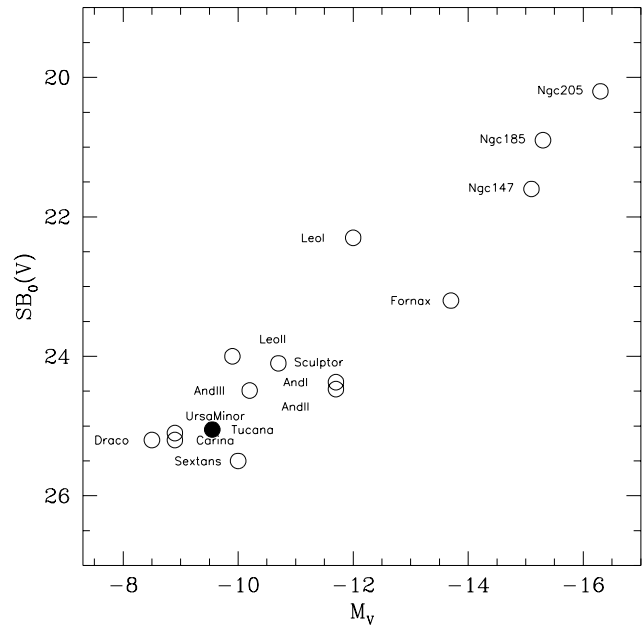


Fig. 15. Central surface brightness vs. absolute V magnitude for LG dwarf spheroidals

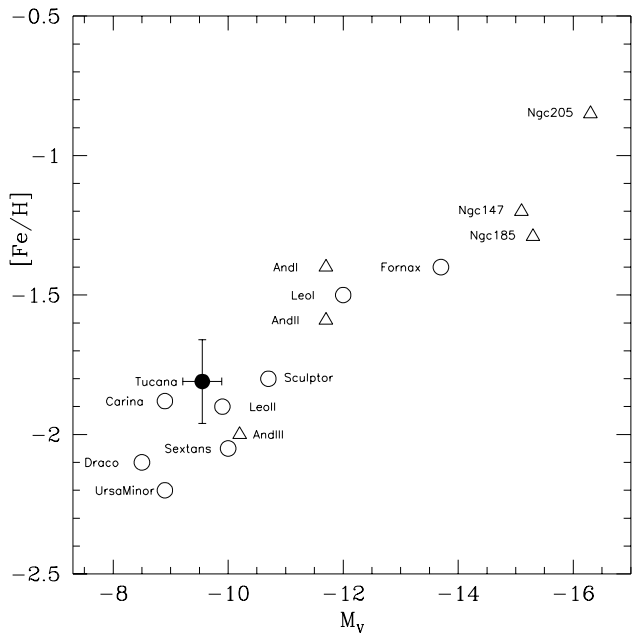


Fig. 16. The metallicity–luminosity relation defined by the dSph companions of the Galaxy (open circles) and of M31 (open triangles). Tucana (full dot) obeys to the same relation

an intrinsic property of dSph's, not related to proximity to a bigger galaxy. Since surface density probably reflects the evolution of dwarfs through mass loss, the implication would be that gas loss is more dependent on intrinsic galaxy properties (e.g., mass) than on interaction with environment.

Bellazzini et al. (1996) have recently proposed that the central surface brightnesses of the dwarf spheroidal satellites of the Milky Way are correlated with their Galactocentric distance, in the sense that dwarfs closer to the Galactic Center are dimmer. An even tighter bivariate correlation is found between surface brightness and a linear combination of distance and absolute magnitude, which seems to hold also for the M31 dSph satellites. This may imply that their structure is influenced by the environment. Having a "normal" central surface brightness for its absolute luminosity, and a large galactocentric distance, Tucana clearly deviates from their proposed correlation. It is not clear whether the Bellazzini's et al. (1995) trends mainly reflect a correlation between R_{GC} with luminosity. In addition, it must be kept in mind that selection effects may be operating against the discovery of dim dwarfs at large distances.

This study confirms that Tucana has a low metallicity: this distant, isolated dwarf follows (Fig. 16) the metallicity-luminosity relation defined by the M31 and Milky Way dSph companions (Caldwell et al. 1992). This is a further evidence that formation and evolution of the dSph's is not strongly influenced by the environment (cf. Armandroff 1994 and references therein). As the metallicity appears to be a function of luminosity only, the metal enrichment process itself seems not to be influenced by the presence of a nearby galaxy (Da Costa 1994). Does the metallicity of Tucana imply self-enrichment with some retention and/or re-capture of gas (Silk, Wyse, & Shields 1987) ? Because of the isolated location of Tucana and the absence of an intermediate-age population, re-capture of gas as an effect of interaction seems unlikely as it is unlikely that the metallicity of this dwarf be influenced by accretion of pre-enriched external material. Thus it may represent an ideal laboratory for studying chemical evolution of dwarf spheroidals.

As a final comment, we note that measuring the radial velocity of Tucana, in addition to the accurate distance given here, will allow to use this isolated galaxy as a test particle to constrain the mass distribution and dynamics of the Local Group (Zaritsky 1994). Moreover, obtaining high-precision velocities for the brightest giants in Tucana, to measure the internal velocity dispersion of Tucana and infer its dark matter content, would be a valuable task for a 10-metre class telescope.

Acknowledgements. I.S. acknowledges support by MURST during his "Dottorato di Ricerca" fellowship. We thank Dr. J. Bahcall for providing the computer code of his models, Dr. G. Clementini for sharing her extinction measurements, and the La Silla observatory staff for support. E.H. wishes to thank Jeremy Mould for useful conversations regarding dwarf galaxies.

References

Aaronson M., Mould J., 1985, ApJ 290, 191

Armandroff T.E., 1994. In: Layden A., Smith R.C., Storm J. (eds) Proc. 3rd CTIO/ESO Workshop, The LG: Comparative and Global Properties. ESO, Garching, p. 211

Armandroff T.E., Da Costa G.S., Caldwell N., Seitzer P., 1993, AJ 106, 986

Bahcall J. N., 1986, ARA&A 24, 577

Bahcall J.N., Soneira R.M., 1980, ApJS 44, 73

Bellazzini M., Fusi Pecci F., Ferraro F. R., 1996, MNRAS, in press

Bergbush P.A., VandenBerg D.A., 1992, ApJS 81, 163

Bressan A., Chiosi C., Fagotto F., 1994, ApJS 94, 63

Burstein D., Heiles C., 1982, AJ 87, 1165

Caldwell N., 1995, in Fresh Views of Elliptical Galaxies, ASP Conf. Ser. No.86 (San Francisco, ASP), eds. A. Buzzoni, A. Renzini and A. Serrano, in press

Caldwell N., Armandroff T.E., Seitzer P., Da Costa G.S., 1992, AJ 103, 840

Carraro G., Chiosi C., Bressan A., Bertelli G., 1994, A&AS, 103, 375

Castellani M., Marconi G., Buonanno R., 1995. In: Formation of the Galactic Halo...Inside and Out (in press)

Corwin Jr. H.G., de Vaucouleurs G., de Vaucouleurs A., 1985, Southern Galaxy Catalog (University of Texas Press, Austin, TX)

Da Costa G.S., 1992. In: Barbuy B., Renzini A. (eds) Proc. IAU Symp. 149, The Stellar Populations of Galaxies. Kluwer, Dordrecht, p. 191

Da Costa G.S., 1994. In: Meylan G., Prugniel P. (eds) Proc. of ESO Workshop 49, Dwarf Galaxies. ESO, Garching, p. 221

Da Costa G.S., Armandroff T.E., 1990, AJ 100, 162 (DA90)

Demers S., Irwin M.J., 1993, MNRAS 261, 657

Djorgovski, S., 1993, ASP Conf. Ser. 50, 373

Ferguson H.C., Binggeli B., 1994, A&R 6, 67

Freedman W. L., 1994. In: Layden A., Smith R.C., Storm J. (eds) Proc. 3rd CTIO/ESO Workshop, The LG: Comparative and Global Properties. ESO, Garching, p. 211

Gallagher J. S., Wyse R. F. G., 1994, PASP, 106, 1225

Gallart C., Aparicio A., Chiosi C., Bertelli G., Vilchez M., 1994, ApJ 425, L9

Girardi L., Bressan A., Chiosi C., Bertelli G., Nasi E., 1996, A&AS, in press

Held E.V., Mould J.R., 1994, AJ 107, 1307

Ibata R.A., Gilmore G., Irwin M.J., 1994, Nature 370, 194

Kurucz R. L., 1991. In: A.G. Davis Philip, A.G. Upgren, K.A. Janes (eds), Precision Photometry: Astrophysics of the Galaxy. L.Davis Press, Schenectady, p.27

Landolt A.U., 1992, AJ 104, 340

Lavery R.J., Michell K.J., 1992, AJ 103, 81

Lavery R.J., 1990, IAU Circular No. 5139

Lee M.G., Freedman W.L., Madore B.F., 1993a, ApJ 417, 553

Lee M.G., Freedman W.L., Mateo M., et al., 1993b, AJ 106, 1420

Lehnert M.D., Bell R.A., Hesser J.E., Oke J.B., 1992, ApJ 395, 466

Madore B.F., Freedman W.L., 1995, AJ 109, 1645

Mould J.R., Da Costa G.S., 1988. In: Blanco V.M., Phillips M.M. (eds) ASP Conf. Ser. 1, Progress and Opportunities in Southern Hemisphere Optical Astronomy. ASP, San Francisco, p.197

Mould J. R., Kristian J., 1986, ApJ 305, 591

Sagar R., Hawkins M.R.S., Cannon R.D., 1990, MNRAS 242, 167

Sandage A.R., 1954, AJ 59, 162

Savage B.D., Mathis J.S., 1979, ARA&A 17, 73

Silk J., Wyse R.F.G., Shields G.A., 1987, ApJ 322, L59

Smecker-Hane T.A., Stetson P.B., Hesser J.E., Lehnert M.D.,
 1994, AJ 108, 507

Stetson P.B., 1987, PASP 99, 191

Stetson P.B., 1994, PASP 106, 250

Suntzeff N.B., Mateo M., Terndrup D.M., et al., 1993, ApJ
 418, 208

Tyson J.A., 1988, AJ 96, 1

van den Bergh S., 1994, ApJ 428, 617

Veronesi C., 1995, *Laurea Thesis*, University of Padova

Zaritsky D., 1994. In: Layden A., Smith R.C., Storm J. (eds)
 Proc. 3rd CTIO/ESO Workshop, The LG: Comparative
 and Global Properties. ESO, Garching, p. 211

Zinn R., 1993. In: Smith G.H., Brodie J.P. (eds), ASP Conf.
 Ser. 48, The Globular Cluster-Galaxy Connection. ASP,
 San Francisco, p.302

Zinn R., West M.J., 1984, ApJS 55, 45